Green Synthesis of Zinc Nanoparticles Using Aqueous Extract of Magnoliae officinalis and Assessment of its Bioactivity Potentials

Article *in* Biointerface Research in Applied Chemistry · July 2020

DOI: 10.33263/BRIAC111.77657774

6 authors, including:

Maryam Karkhane
Shahid Beheshti University of Medical Sciences
40 PUBLICATIONS **112** CITATIONS

SEE PROFILE

A. Marzban
Lorestan University of Medical Sciences
47 PUBLICATIONS **119** CITATIONS

SEE PROFILE

Biointerface Research in Applied Chemistry
Platinum Open Access Journal (ISSN: 2069-5837)

Article
Volume 11, Issue 1, 2021, 7765 - 7774
https://doi.org/10.33263/BRIAC111.77657774

Green Synthesis of Zinc Nanoparticles Using Aqueous Extract of *Magnoliae officinalis* and Assessment of its Bioactivity Potentials

Farhad Gilavand [1], Reyhaneh Saki [1], Seyedeh Zahra Mirzaei [2], Hamed Esmaeil Lashgarian [3], Maryam Karkhane [3], Abdolrazagh Marzban [2,*]

[1] Department of Microbiology, Islamic Azad University, Khorramabad Branch, Khorramabad, Iran; farhadgilavand1359@gmail.com (F.G.); Reyhaneh_S@yahoo.com (R.S.);
[2] Razi Herbal Medicines Research Center, Lorestan University of Medical Sciences, Khorramabad, Iran; zahramirzaei1.1990@gmail.com (S.Z.M.);
[3] Department of Medical Biotechnology, School of Medicine, Lorestan University of Medical Sciences, Khorramabad, Iran; Maryam_karkhane@hotmail.com (M.K.); hamedesmaiili@gmail.com (H.E.L.);
* Correspondence: marzban86@gmail.com;

Scopus Author ID 55860483200
Received: 24.05.2020; Revised: 29.06.2020; Accepted: 30.06.2020; Published: 3.07.2020

Abstract: Today, considerable attention has been drawn to the unique physicochemical and biological properties of zinc nanoparticles. In this study, ZnO-NPs were synthesized using *Magnoliae officinalis* (MO) aqueous extract as a reducing and capping agent. Characteristics of ZnO-NPs were analyzed using analytical techniques such as UV, FTIR, SEM, XRD, EDX, DLS, and zeta potential. After that, the antibacterial activity of ZnO-NPs against methicilin resistant *Staphylococcus aureus* (MRSA) was studied. The results of FTIR and UV-vis spectra showed successful biosynthesis of ZnO-NPs, because the absorption peaks and functional groups involved in the synthesis process were well developed. Additionally, the SEM micrograph and the DLS showed that the morphology and size distribution of the ZnO-NPs were spherical with a size of 150 nm. XRD, EDX, and zeta potential indicated crystal form of ZnO-NPs with zinc: oxygen ratio of 72.35:27 and a surface charge of +28 mv. The antibacterial activity of ZnO-NPs with the assessment of the well-diffusion method, MIC and MBC indicated the highest inhibitory effect at a concentration of 300 µg/ml, MIC 250 µg/ml and MBC 300 µg/ml. As regards the desirable antimicrobial activity of biosynthesized ZnO-NPs using MO extract, they may be used for medicinal purposes, in particular as antimicrobials and antiseptic agents.

Keywords: Zinc oxide nanoparticles; *Magnoliae officinalis*; Green synthesis; *Staphylococcus aureus* (MRSA).

1. Introduction

Nanomaterials are nanoparticles (NPs) with unique characteristics distinct from their bulk chemicals. Nanomaterials have typically demonstrated enhanced catalytic reactivity, strong thermal conductivity, nonlinear optical performance, and high chemical stability due to the large surface area ratio [1, 2]. With the development of nanoparticle synthesis approaches, their application in various fields, such as agriculture, medicine, cosmetics, the environment, and chemistry, has extended [3, 4]. Numerous methods have been developed to fabricate metallic NPs, the most widely used of which include chemical reduction, microwave methods, and thermal deposition [5, 6]. Many of these methods use toxic compounds to synthesize NPs

or use a great deal of energy to perform the synthesis. Therefore, green synthesis is an alternative way to produce more beneficial NPs using plant metabolites, microorganisms, and algae. Green synthesis has numerous advantages, such as minimizing the use of dangerous chemicals, biocompatibility, low toxicity, simplicity of processing, cost-effectiveness, and the potential to monitor the synthesis process [7].

Infections caused by emerging hospital infections are a severe problem for the treatment of infectious diseases [8]. MRSA pathogens are known to be an important challenge worldwide. As MRSA strains are resistant to many current antibiotics, new antimicrobial compounds are required to overcome this issue [9, 10].

Nanoparticle-based antimicrobial compounds (nanobiotics) are one of the most effective strategies to fight antibiotic-resistant bacteria. Synthetic NPs using medicinal plants can ameliorate the side effects of them [11]. On the other hand, the use of plant metabolites with antimicrobial properties increases the efficiency of NPs. Studies have shown that Magnolol and Honokiol, the main components of *M. officinalis* (MO) induce antibiotic susceptibility in MRSA strains by suppressing resistance genes [12].

In this study, the feasibility of ZnO-NP synthesis was conducted using *M. officinalis* aqueous extract for the first time. Then, the antibacterial efficacy of biosynthetic NPs against methicillin-resistant *S. aureus* (MRSA) was investigated.

2. Materials and Methods

2.1. Plant materials and extract preparation.

To prepare MO extract, 10 g of dried bark powder was poured into a 250 ml Erlenmeyer flask containing 100 ml of distilled water. The flask was then sonicated in a bath sonicator at 45 °C for 1 h. After that, the extract was filtered by Whatman filter paper (no. 1), and the resulting filtrate was used as a reducing and capping for NPs synthesis.

2.2. Green synthesis of ZnO-NPs.

To fabricate ZnO-NPs, 90 ml of $Zn(NO_3)_2.6H_2O$ solution (0.01 M) in a 100 ml flask was placed on hotplate magnetic stirrer. Approximately 10 ml of aqueous extract was added drop-wise to the sample flask under constant stirring at room temperature until the clear solution changed to pale yellow. The mixture was then kept at 70 °C for 2 h until ZnO-NPs were formed entirely. The precipitate was harvested by centrifugation at 12000 rpm and washed twice with deionized water and dried in an oven at 50 °C. The dried powder was stored for further studies.

2.3. ZnO-NPs characterization.

The physicochemical properties of biosynthesized ZnO-NPs (The fine powder) were studied through analytical methods including Uv-visible (Jenway 6310; Japan), FTIR (Thermo AVATAR; USA), XRD (XRD Philips PW1730; Netherlands), FE-SEM-EDAX (TESCAN MIRA3; Czech Republic), and DLS-Zeta potential (Zetasizer Nano ZS90, Malvern, UK).

2.4. Antibacterial activity of ZnO-NPs.

2.4.1. Well-diffusion assay.

Antibacterial activity of MO extract and biosynthesized ZnO-NPs were examined against Methicillin-resistant *Staphylococcus aureus* (MRSA) (ATCC 33591) by well diffusion method on Muller Hinton agar (MHA) plates [13]. The MRSA strain was purchased from the Iranian Research Organization for Science and Technology (IROST). Prior to use, the MO extract and Zn-NPs were filtered using 0.45 filter paper. A fresh culture of *S. aureus* (MRSA) was prepared at a cell density of 0.5×10^8 CFU/mL as 0.5 Mc Farland standard in phosphate buffer saline. Bacterial cells spread with a sterile cotton swab on the agar plate. Afterward, 6 mm wells were created with a sterile metal cork borer in agar. Twenty microliters of different concentrations of MO extract and ZnO-NPs were added to each well. Chloramphenicol (30 µg/well) was used as a positive control. The plates were incubated at 37 °C for 24 h. Antimicrobial activity was expressed in terms of creating growth inhibition halos around the wells.

2.4.2. MIC and MBC assessments.

Minimum inhibitory concentration (MIC) was determined using the microdilution method according to Clinical and Laboratory Standards Institute guidelines (CLSI). Serial dilutions of the MO extract and ZnO-NPs solutions were prepared for achieving different concentrations. One milliliter of each dilution was added to 4 ml Muller Hinton broth (MHB) in the sterile glasses. Fresh culture cells (100 µl) with an optical density of 0.5 Mc Farland were inoculated to each tube. The test tubes and control (untreated) were incubated for 24 h at 37 °C. After that, the bacterial growth was tracked by measuring the optical density at 600 nm using the UV-vis spectrophotometer. To determine the minimum bactericidal concentration (MBC), those tubes that display no bacterial growth were cultured on MHA plates and incubated for 24 h at 37 °C.

3. Results and Discussion

3.1. Uv-visible spectroscopy.

The biosynthesis of ZnO-NPs using MO extract was determined by changing the solution's color from brown to pale yellow. Because the color of the ZnO-NPs was white and the MO extract was dark brown, it was not possible to confirm the ZnO-NPs by discoloring the solution. However, the discoloration may indicate the effective processing of ZnO-NPs by MO extract. Figure 1A and B show the UV-Vis spectra of ZnO-NPs and MO extract, respectively. As seen in Figure 1B, a known adsorption signal at 371.25 nm is attributed to the formation of ZnO-NPs [14]. According to studies, the Uv adsorption peaks of ZnO-NPs often appears in the range of 300-380 nm. This range is related to the transfer of electrons from voltage to the conduction band involved in the formation of ZnO-NPs [15]. Towards the other side, the MO extract spectrum has a variety of peaks which do not occur in the ZnO-NPs region. It can be concluded, therefore, that the purity of the synthesized ZnO-NPs by the extract was appropriate.

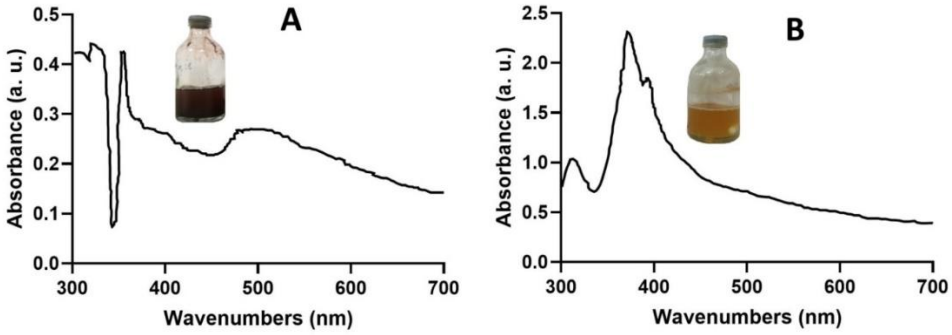

Figure 1. UV-Vis spectra of A and B show absorbance intensity of MO extract and biosynthesized ZnO-NPs, respectively.

3.2. SEM and EDX studies.

SEM and EDX were used to study morphology and elemental analysis of NPs. As shown in Figure 2, ZnO-NPs were slightly aggregated together. Additionally, spherical NPs can be seen throughout the field with an approximate size of 50-150 nm. On the other hand, morphological analysis of NPs indicates their amorphous feature. Figure 3b shows the EDX spectrum of ZnO-NPs that three distinct peaks at 1.1 kV, 8.6 kV, and 9.5 kV related to the elemental proportion of the ZnO-NPs [16]. According to data from the EDX spectrum, the ratio of the constituent elements of ZnO-NPs was measured at approximately 72.35% and 27% for zinc and oxygen, respectively.

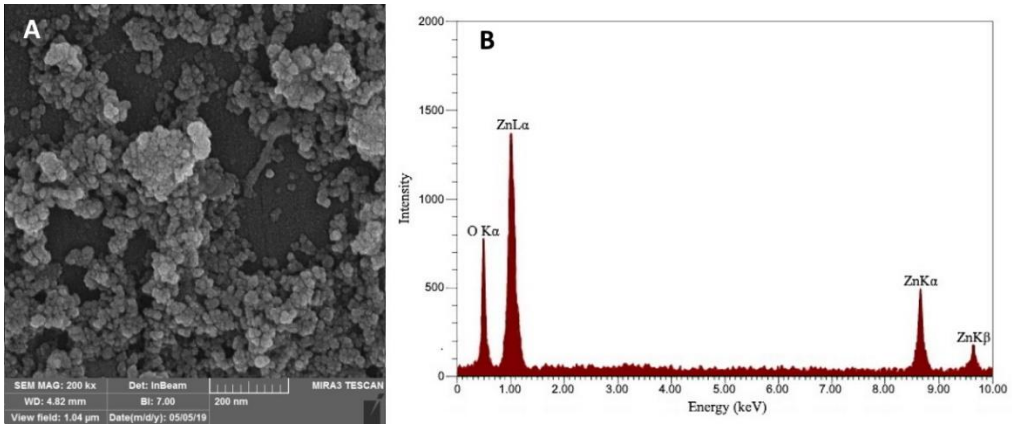

Figure 2. Electron microscopy analysis of biosynthesized ZnO-NPs. A) FESEM micrograph, B) EDX spectrum.

3.3. FTIR analysis.

FTIR spectroscopy was performed to identify active functional groups involved in the formation of ZnO-NPs in the range of 600-4000 nm. According to the spectra presented in Figure 3, broad and stretching peaks at 3339.21 and 2141.23 nm can be attributed to the hydroxyl and alkyl groups, respectively, in bioactive compounds of MO extract [17]. Two peaks in 1841.12 and 1289.34 indicate the presence of Alken, Carbonyl, and Hydroxyl groups in reducing sugars [18]. Additionally, the peaks of 3419.24 and 3038.07 nm in the ZnO-NPs spectrum demonstrate the role of hydroxyl and carboxylic groups on the formation of NPs. Other peaks in 1699.05 and 1427.32 regions also indicate the changes in the functional groups of the compounds in MO extract after the formation of ZnO-NPs [19].

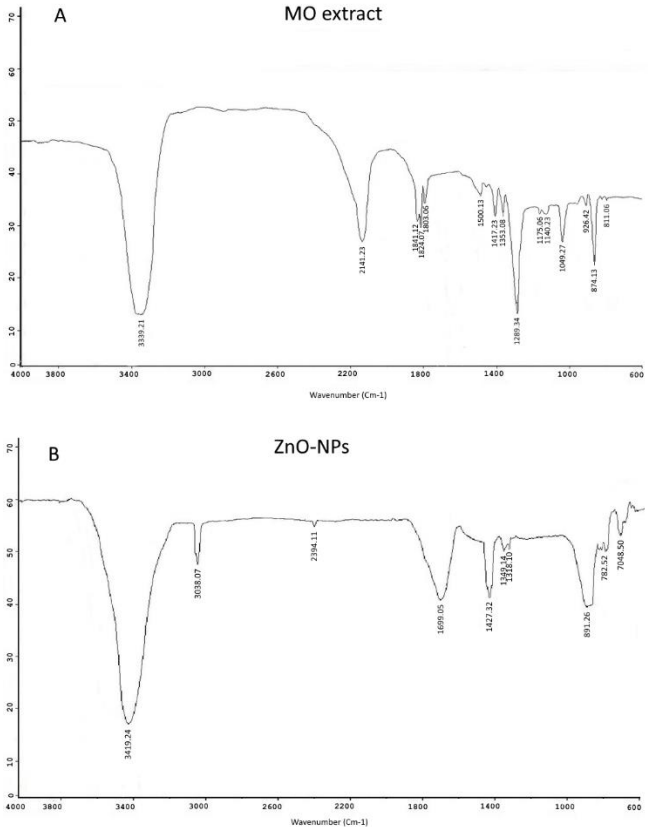

Figure 3. FTIR spectra of A) MO extract and biosynthesized ZnO NPs.

3.4. DLS and Zeta potential studies.

DLS analysis was used to evaluate the hydrodynamic diameter and size distribution of ZnO-NPs. Figure 4A shows the particle size distribution so that the graph peak of the ZnO-NPs was approximately 150 nm. The distribution range of NPs varies from 50 to 750 nm, indicating that part of the NPs is aggregated. Such findings were compatible with the SEM image. In addition, the PDI value was about 0.66, meaning that ZnO-NPs have a heterogeneous distribution. Studies have shown that the hydrodynamic diameter of NPs may be affected by plant metabolites. Polyphenolic compounds cap the NPs and thereby prevent them from aggregation [20, 21].

The zeta potential of NPs can also play a critical role in their biological activity. Figure 4B shows the surface load of NPs in the positive range. The maximum surface charge of NPs was about +28 mv. Since research has been demonstrated that high-stability NPs have a surface charge between +10 and -10, heterogeneity in the particle size caused by predictive aggregation was predictable [22].

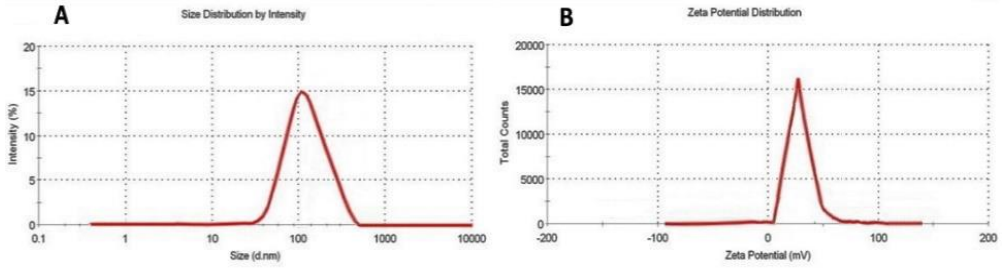

Figure 4. A) Particle size distribution (DLS) and B) surface charge distribution (Zeta potential) of biosynthesized ZnO-NPs.

3.5. XRD analysis.

X-ray diffraction analysis (XRD) was used to investigate the crystalline phase of NPs. XRD crystallography of ZnO-NPs was performed by Philips PW1730 XRD with a copper source (Kα = 1.54.) From 20 to 80 at C at 2. C. Figure 5 shows the XRD pattern of NPs as plates (100), (002), (101), (102), (110), (103), (112) and (201) based on normal angles (2θ) of 31.18, 35.16, 37.06, 46.51, 57.58, 64.11, 67.47 and 69.23, respectively [23]. The size of the crystals was determined on the basis of the Scherrer formula of approximately 145 nm.

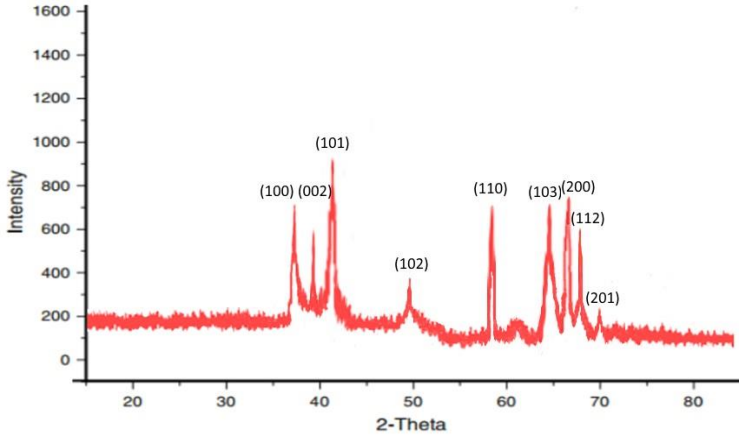

Figure 5. The X-ray diffraction (XRD) pattern of biosynthesized ZnO-NPs.

3.6. Antibacterial activity studies.

The antibacterial assay results using the Well diffusion technique displayed more effective inhibition at 300 µg/ml of ZnO-NPs than the MO extract at 500 µg/ml (Figure 6).

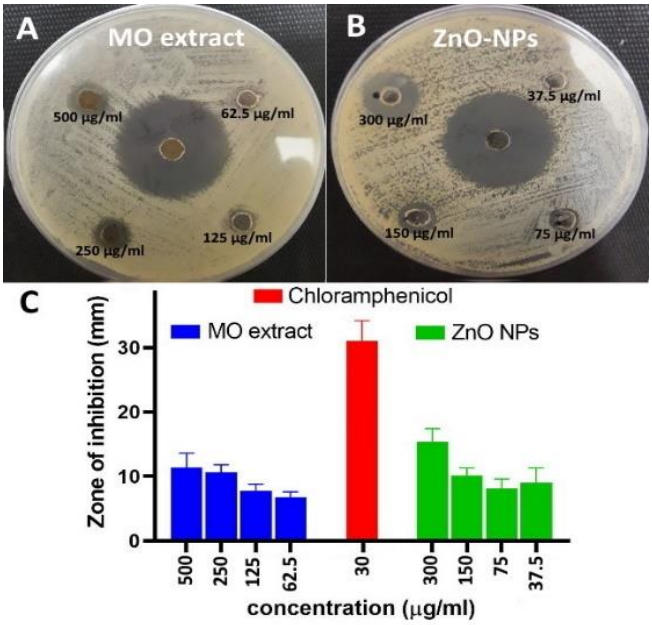

Figure 6. Antibacterial activity assay of A) MO extract B) ZnO-NPs against MRSA strain (ATCC 33591) and C) diameters of growth inhibition halos at the presence of different concentrations of MO extract and ZnO-NPs.

As can be seen in figure 7, the MIC values for ZnO-NPs and MO extract were determined at 250 and 625 µg/ml, respectively. MBC values were determined after the MIC assay that for ZnO-NPs and MO were estimated 300 and 900 µg/ml.

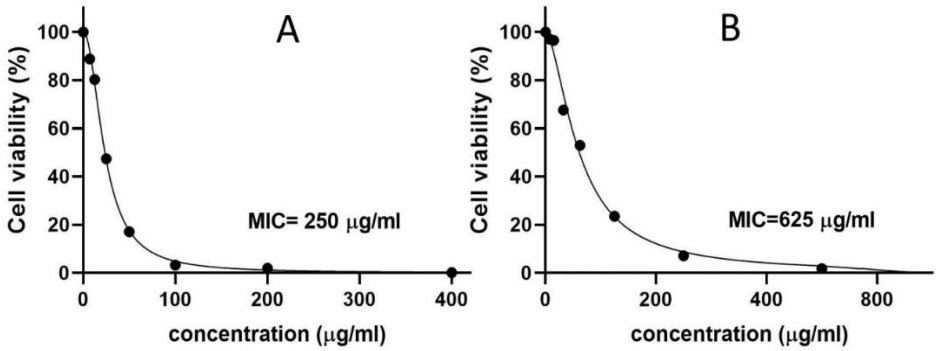

Figure 7. Cell viability based on MIC values. The percentage of living cells in the presence of serial dilutions of MO extract and ZnO-NPs.

The two major compounds found in MO extract, namely honokiol and magnolol, exhibited potent biological properties [24]. In this regard, Kim et al. (2015) showed that magnolol and honokiol have robust growth inhibition activity against MRSA [12]. Ha et al. (2019) showed the inhibitory potential of MO metabolites against *S. aureus*, *E. coli*, *Candida albicans* [25]. Zheng et al. (2019) synthesized gold nanoparticles using MO aqueous extract, which demonstrated significant anti-cancer activity against the lung cancer line (A549) [26].

In the process of NPs synthesis by MO extract, the role of phytochemicals as reducing and capping agents is prominent [1, 27]. Therefore, the biological activity of NPs is consistent with the type of compounds present in the extract and their bioactive properties. Additionally, the morphological and reactive properties of NPs are also affected by capping and stabilizing agents [5]. Metallic NPs with significant biological activity has been introduced as a new type of antimicrobials. ZnO-NPs have clearly shown that they have great potential to inhibit a variety of pathogens [13]. The mechanism of action of the antimicrobial effect of ZnO-NPs appears to be complicated, with variation in targeting against microbes [28]. Studies have shown that ZnO-NPs bind to bacterial cells, disrupting the plasma membrane integrity and altering its permeability. Hydrogen peroxide and other oxygen free radicals are the most important mediators produced under the influence of ZnO-NPs. Therefore, the production of multiple reactants by ZnO-NPs increases its antimicrobial properties [14]. On the other hand, surface charge and size are considered to be critical factors in the antimicrobial capacity of NPs. Positively charged NPs are more likely to bind to bacteria and therefore have a higher lethality [29]. In this study, biosynthesized ZnO-NPs by MO extract had a positive charge (+28 mv) and showed potent antimicrobial activity against *S. aureus* (MRSA). The size of NPs is an effective factor in their biological activity. As confirmed in the previous studies, small NPs with high monodispersity exhibit greater efficacy to penetrate the cells [30]. In contrast, polydispersed NPs have stronger photocatalytic activity as well as good reactive agents for the production of intermediate oxygen radicals [31]. In this study, ZnO-NPs had an average size of about 150 nm, which can be a suitable reactor for catalyzing oxidation reactions and have a high capacity for intermediate oxygen production.

4. Conclusions

The physicochemical properties of ZnO-NPs showed successful biosynthesis by MO extract with substantial antimicrobial potential. As mentioned, green synthesis methods are biocompatible and cost-effective. *Magnoliae officinalis* is known to have metabolites with potent biological activities. Thus, MO metabolites involved in the green synthesis of NPs can

improve antimicrobial activity, biocompatibility, and sustainability. In this study, the use of the MO extract to synthesize ZnO-NPs, as expected, increased their antibacterial potential. Taken together, the biosynthetic ZnO-NPs can be used for medicinal purposes, especially as antimicrobials and disinfectants.

Funding

This research was a part of the thesis to receive a Master of Science (Ms.C) in Faculty of Basic Sciences, Department of Microbiology, Islamic Azad University, Khorramabad branch. No formal financial support has received for this research.

Acknowledgments

This research was performed in Razi Herbal Medicines Research Center, Lorestan University of Medical Sciences.

Conflicts of Interest

The authors declare no conflict of interest.

References

1. Nasab, N.K.; Dehnad, A.R.; Salimizand, H.; Taherzadeh, D.; Prakash, D.; Verma, K.; Darroudi, M. Zinc selenide nanoparticles (ZnSe-NPs): Green synthesis and investigation of their cytotoxicity effects. *Ceramics International* **2016**, *42*, 12115-12118, https://doi.org/10.1016/j.ceramint.2016.04.143.
2. Jayabalan, J.; Mani, G.; Krishnan, N.; Pernabas, J.; Devadoss, J.M.; Jang, H.T. Green biogenic synthesis of zinc oxide nanoparticles using *Pseudomonas putida* culture and its In vitro antibacterial and anti-biofilm activity. *Biocatalysis and Agricultural Biotechnology* **2019**, *21*, https://doi.org/10.1016/j.bcab.2019.101327.
3. Dhandapani, K.V.; Anbumani, D.; Gandhi, A.D.; Annamalai, P.; Muthuvenkatachalam, B.S.; Kavitha, P.; Ranganathan, B. Green route for the synthesis of zinc oxide nanoparticles from *Melia azedarach* leaf extract and evaluation of their antioxidant and antibacterial activities. *Biocatalysis and Agricultural Biotechnology* **2020**, *24*, https://doi.org/10.1016/j.bcab.2020.101517.
4. Gholami, M.; Shahzamani, K.; Marzban, A.; Lashgarian, H.E. Evaluation of antimicrobial activity of synthesised silver nanoparticles using *Thymus kotschyanus* aqueous extract. *IET nanobiotechnology* **2018**, *12*, 1114-1117, https://doi.org/10.1049/iet-nbt.2018.5110.
5. Chandra, H.; Kumari, P.; Bontempi, E.; Yadav, S. Medicinal plants: Treasure trove for green synthesis of metallic nanoparticles and their biomedical applications. *Biocatalysis and Agricultural Biotechnology* **2020**, *24*, https://doi.org/10.1016/j.bcab.2020.101518.
6. Habtemariam, A.B.; Sibhatu, A.K.; Weldegebrieal, G.K.; Zelekew, O.A.; Tekletsadik, B.T. Bio-mediated synthesis of ZnO nanostructures from *Thymus Schimperi* leaves extract and its antibacterial and photocatalytic activities. *Letters in Applied NanoBioScience* **2020,** *9*, 808-813. https://doi.org/10.33263/LIANBS91.808813.
7. Khosravi-Darani, K.; Gomes da Cruz, A.; Shamloo, E.; Abdimoghaddam, Z.; Mozafari, M.R. Green synthesis of metallic nanoparticles using algae and microalgae. *Letters in Applied NanoBioScience* **2019**, *8*, 666-670. https://doi.org/10.33263/LIANBS83.666670.
8. Karkhane, M.; Pourhoseingholi, M.A.; Kimiia, Z.; Mortazavi, S.M.; Akbariyan Torkabad, M.R.; Hossieni Aghdam, S.K.; Marzban, A.; Zali, M.R. Attitudes toward nosocomial infections associated mortality at intensive care units, and evaluation of the risk factors. *Archives of Clinical Infectious Diseases* **2016**, *11*, https://doi.org/10.5812/archcid.22504.
9. Zhou, K.; Li, C.; Chen, D.; Pan, Y.; Tao, Y.; Qu, W.; Liu, Z.; Wang, X.; Xie, S. A review on nanosystems as an effective approach against infections of *Staphylococcus aureus*. *International Journal of Nanomedicine* **2018**, *13*, 7333-7347, https://doi.org/10.2147/IJN.S169935.
10. Ebrahimipour, G.; Moradi, A.; Mehrdad, M.; Marzban, A.; Alaee, H. Evaluation of antimicrobial substance produced by a bacterium isolated from *Parmacella iberica*. *Jundishapur Journal of Microbiology* **2011**, *4*,131-140.
11. Hameed, S.; Iqbal, J.; Ali, M.; Khalil, A.T.; Abbasi, B.A.; Numan, M.; Shinwari, Z.K. Green synthesis of zinc nanoparticles through plant extracts: establishing a novel era in cancer theranostics. *Materials Research Express* **2019**, *6*:102005, https://doi.org/10.1088/2053-1591/ab40df.

12. Kim, S.Y.; Kim, J.; Jeong, S.I.; Jahng, K.Y.; Yu, K.Y. Antimicrobial effects and resistant regulation of magnolol and honokiol on methicillin-resistant *Staphylococcus aureus*. *BioMed Research International* **2015**, *2015*, https://doi.org/10.1155/2015/283630.
13. Banerjee, S.; Vishakha, K.; Das, S.; Dutta, M.; Mukherjee, D.; Mondal, J.; Mondal, S.; Ganguli, A. Antibacterial, anti-biofilm activity and mechanism of action of Pancreatin doped Zinc oxide nanoparticles against methicillin resistant *Staphylococcus aureus*. *Colloids and Surfaces B: Biointerfaces* **2020**, *190*, https://doi.org/10.1016/j.colsurfb.2020.110921.
14. Pandimurugan, R.; Thambidurai, S. Novel seaweed capped ZnO nanoparticles for effective dye photodegradation and antibacterial activity. *Advanced Powder Technology* **2016**, *27*, 1062-1072, https://doi.org/10.1016/j.apt.2016.03.014.
15. Murugan, K.; Roni, M.; Panneerselvam, C.; Aziz, A.T.; Suresh, U.; Rajaganesh, R.; Aruliah, R.; Mahyoub, J.A.; Trivedi, S.; Rehman, H.; Naji Al-Aoh, H.A.; Kumar, S.; Higuchi, A.; Vaseeharan, B.; Wei, H.; Senthil-Nathan, S.; Canale, A.; Benelli, G. *Sargassum wightii*-synthesized ZnO nanoparticles reduce the fitness and reproduction of the malaria vector Anopheles stephensi and cotton bollworm Helicoverpa armigera. *Physiological and Molecular Plant Pathology* **2018**, *101*, 202-213, https://doi.org/10.1016/j.pmpp.2017.02.004.
16. Ebadi, M.; Zolfaghari, M.R.; Aghaei, S.S.; Zargar, M.; Shafiei, M.; Zahiri, H.S.; Noghabi, K.A. A bio-inspired strategy for the synthesis of zinc oxide nanoparticles (ZnO NPs) using the cell extract of cyanobacterium Nostoc sp. EA03: from biological function to toxicity evaluation. *RSC advances* **2019**, *9*, 23508-23525, https://doi.org/10.1039/C9RA03962G.
17. Ashrafi, B.; Rashidipour, M.; Marzban, A.; Soroush, S.; Azadpour, M.; Delfani, S.; Ramak, P. *Mentha piperita* essential oils loaded in a chitosan nanogel with inhibitory effect on biofilm formation against S. mutans on the dental surface. *Carbohydrate polymers* **2019**, *212*, 142-149, https://doi.org/10.1016/j.carbpol.2019.02.018.
18. Gilavand, F.; Marzban, A.; Ebrahimipour, G.; Soleimani, N.; Goudarzi, M. Designation of chitosan nano-vaccine based on MxiH antigen of *Shigella flexneri* with increased immunization capacity. *Carbohydrate Polymers* **2020**, *232*, https://doi.org/10.1016/j.carbpol.2019.115813.
19. Hemanth Kumar, N.K.; Andia, J.D.; Manjunatha, S.; Murali, M.; Amruthesh, K.N.; Jagannath, S. Antimitotic and DNA-binding potential of biosynthesized ZnO-NPs from leaf extract of *Justicia wynaadensis* (Nees) Heyne - A medicinal herb. *Biocatalysis and Agricultural Biotechnology* **2019**, *18*, https://doi.org/10.1016/j.bcab.2019.101024.
20. Sirdeshpande, K.D.; Sridhar, A.; Cholkar, K.M.; Selvaraj, R. Structural characterization of mesoporous magnetite nanoparticles synthesized using the leaf extract of *Calliandra haematocephala* and their photocatalytic degradation of malachite green dye. *Applied Nanoscience* **2018**, *8*, 675-683, https://doi.org/10.1007/s13204-018-0698-8.
21. Telgmann, L.; Nguyen, M.T.K.; Shen, L.; Yargeau, V.; Hintelmann, H.; Metcalfe, C.D. Single particle ICP-MS as a tool for determining the stability of silver nanoparticles in aquatic matrixes under various environmental conditions, including treatment by ozonation. *Analytical Bioanalytical Chemistry* **2016**, *408*, 5169-5177, https://doi.org/10.1007/s00216-016-9685-7.
22. Keller, A.A.; Wang, H.; Zhou, D.; Lenihan, H.S.; Cherr, G.; Cardinale, B.J.; Miller, R.; Ji, Z. Stability and aggregation of metal oxide nanoparticles in natural aqueous matrices. *Environmental Science Technology* **2010**, *44*, 1962-1967, https://doi.org/10.1021/es902987d.
23. Reyes-Torres, M.A.; Mendoza-Mendoza, E.; Miranda-Hernández, Á.M.; Pérez-Díaz, M.A.; López-Carrizales, M.; Peralta-Rodríguez, R.D.; Sánchez-Sánchez, R.; Martinez-Gutierrez, F. Synthesis of CuO and ZnO nanoparticles by a novel green route: Antimicrobial activity, cytotoxic effects and their synergism with ampicillin. *Ceramics International* **2019**, *45*, 24461-24468, https://doi.org/10.1016/j.ceramint.2019.08.171.
24. Luo, H.; Wu, H.; Yu, X.; Zhang, X.; Lu, Y.; Fan, J.; Tang, L.; Wang, Z. A review of the phytochemistry and pharmacological activities of *Magnoliae officinalis* cortex. *Journal of Ethnopharmacology* **2019**, *236*, 412-442, https://doi.org/10.1016/j.jep.2019.02.041.
25. Ha, C.T.T.; Thai, T.H.; Hien, N.T.; Anh, H.T.V.; Diep, L.N.; Thuy, D.T.T.; Nhat, D.D.; Setzer, W.N. Chemical Composition and Antimicrobial Activity of the Leaf and Twig Essential Oils of *Magnolia hypolampra* Growing in Na Hang Nature Reserve, Tuyen Quang Province of Vietnam. *Natural Product Communications* **2019**, *14*, https://doi.org/10.1177/1934578X19860370.
26. Zheng, Y.; Zhang, J.; Zhang, R.; Luo, Z.; Wang, C.; Shi, S. Gold nano particles synthesized from *Magnolia officinalis* and anti-cancer activity in A549 lung cancer cells. *Artificial Cells, Nanomedicine and Biotechnology* **2019**, *47*, 3101-3109, https://doi.org/10.1080/21691401.2019.1645152.
27. Ahmad, S.; Munir, S.; Zeb, N.; Ullah, A.; Khan, B.; Ali, J.; Bilal, M.; Omer, M.; Alamzeb, M.; Salman, S.M.; Ali, S. Green nanotechnology: A review on green synthesis of silver nanoparticles — An ecofriendly approach. *International Journal of Nanomedicine* **2019**, *14*, 5087-5107, https://doi.org/10.2147/IJN.S200254.
28. Gold, K.; Slay, B.; Knackstedt, M.; Gaharwar, A.K. Antimicrobial activity of metal and metal-oxide based nanoparticles. *Advanced Therapeutics* **2018**, *1*, https://doi.org/10.1002/adtp.201700033.

29. Vijayakumar, S.; Mahadevan, S.; Arulmozhi, P.; Sriram, S.; Praseetha, P. Green synthesis of zinc oxide nanoparticles using *Atalantia monophylla* leaf extracts: Characterization and antimicrobial analysis. *Materials Science in Semiconductor Processing* **2018**, *82*, 39-45, https://doi.org/10.1016/j.mssp.2018.03.017.
30. Dimapilis, E.A.S.; Hsu, C.S.; Mendoza, R.M.O.; Lu, M.C. Zinc oxide nanoparticles for water disinfection. *Sustainable Environment Research* **2018**, *28*, 47-56, https://doi.org/10.1016/j.serj.2017.10.001.
31. Gancheva, M.; Markova-Velichkova, M.; Atanasova, G.; Kovacheva, D.; Uzunov, I.; Cukeva, R. Design and photocatalytic activity of nanosized zinc oxides. *Applied Surface Science* **2016**, *368*, 258-266, https://doi.org/10.1016/j.apsusc.2016.01.211.